JPRS-UEQ-89-014
14 NOVEMBER 1989

JPRS Report

Science & Technology

USSR: Engineering & Equipment

JPRS-UEQ-89-014
14 NOVEMBER 1989

SCIENCE & TECHNOLOGY

USSR: ENGINEERING & EQUIPMENT

CONTENTS

UDC 621.311

Controlling the Inductive Power Storage Unit in a Power System

18610541 Novosibirsk IZVESTIYA SIBIRSKOGO OTDELENIYA AKADEMII NAUK SSSR: SERIYA TEKHNICHESKIKH NAUK in Russian No 2, May-Aug 89 pp 113-118

[Article by V. K. Borovik and N. L. Novikov, under the "Problems of Stable Operating Regimes and Optimal Control of Electric Power Systems" rubric: "Controlling an Inductive Energy Storage Unit in a Power System"]

[Text] Disturbances associated with an imbalance in generated and consumed true (active) power are constantly occurring in EES's [electric power systems]. These disturbances have a negative effect on EES's, in that they cause undesired changes in the operating parameters. One of the primary sources of this problem is the disturbance's wide band and the relatively slow high-speed response of the sources of true power being controlled. In order to provide EES's with dynamic and resultative stability while compensating for those major disturbances which occur at high speeds, sometimes, as has been shown for example in [1], some generators must be shut down and consumers have to be cut off, which harms the national economy. Another reason for this situation is is the slow high-speed response of existing sources of active power. At present, low-frequency perturbations are compensated by automatic equipment which operates as described in [2, 3] on boiler and turbine equipment. Installing fast-acting true power sources in EES's would solve a great many problems associated with stability and with the quality of supplied electric power. One such source is the IN [inductive energy storage unit, or power accumulator], which constitutes inductance, including superconducting inductance, and as shown in [4] is connected to an EES through a transformer and a controlling reversible-polarity converter which converts direct current to alternating current.

The effectiveness of the work of the IN in an EES depends both on circuit-operating decisions as well as on the energy storage system used. In many operations, in [4-6] for example, IN's are used both to suppress rotor oscillations in synchronous machines after perturbations, to suppress spontaneous build-ups of current, as well as to equalize generator load schedules so as to improve the economic indicators of power system operation.

This article deals with the development of an IN regulator operating as part of an EES. The first stage in the development of this regulator consisted in determining the efficacy of using an IN to provide EES's with static and dynamic stability, to counter active power disturbances, reduce irregular oscillations, improve load center stability etc. In other words, in those instances when fast-acting true power regulators, one of which is the energy storage unit, are required. The excellent quick response of the energy storage unit, the multifunctionality of its uses in view of the considerable nonlinearities of its characteristics and the transient and nonlinear nature of power generating facilities as elements of the regulating system, are what determine the stringent requirements on the IN regulator.

The specific way any IN operates consists in its limited power consumption which does not, within the law of control, permit the use of deflecting signals in the operating parameters. Thus, within the established operating regime, [7] shows that the exchange between the IN and the power system must be minimal in order to provide the IN with the optimal charge from the standpoint of the maximum active power regulating range. In the transition regimes the power system can be smoothly changed over from one regime to another, taking existing technological and operating conditions into account.

From the above-noted particulars, it follows that IN's should be used to compensate for high-frequency true power disturbances. These requirements can be met by controlling them through the operating parameters carried out. All the above features of an IN have in one way or another been taken into consideration in the development of the regulator. At the first stage, the problem of providing static oscillating stability to a synchronous machine which operates via a power transmission line for a large power system, when an IN has been installed at the tranmitting end of the power transmission line, was examined on a linear model. It should be mentioned that a control parameter such as the voltage frequency used in [5] has a number of well-known drawbacks at the connection point which consist in the complexity of putting the law of control into practice. These complexities stem from existing specifics of the operation of an energy storage unit as part of an EES. This is why the circuit controlling the true generated power return flow through the power transmission lines (P'_{lep}) is used as the primary circuit for regulating the control angle of the power converter thyristors. Regulating the IN both with regard to frequency and P'_{lep} greatly improves the quality of the synchronizing machine's transition processes. When compensating for the reactive power consumed by the energy storage unit's thyristor power converter, the operating regime for the synchronous machine is similar to working directly on a powerful receiving system. This situation can be seen in the areas of stability and to an equal degree in the areas of stability in the realm of control factors for such stabilizing channels of the synchronous machine's disturbance regulator as deflection (k_{0f}) and the derivative (k_{1f}) of the tension of the frequency on the station busbars, as shown in Figure 1. Here, the time constant of the differentiating filter in the regulating channel for derivative P_{lep} may not exceed a value of 0.4 seconds because the

quality of the processes when the value for this constant is further exceeded almost equal the quality of the processes of the synchronous machine operating directly on the buses of a powerful power system.

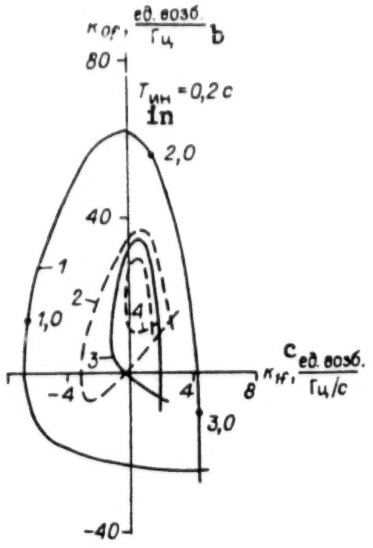

Figure 1. Using an IN [inductive energy storage unit] to suppress synchronous machine oscillations
Key: 2 and 4--without IN; 1 and 3--with IN. Values a,s^{-1} : 0 (1 and 2); --2 (3 and 4). a--logarithmic attenuating decrement; b--disturbance unit/Hz; c--disturbance unit/Hz per second.

Where there are considerable changes in the IN's charge, in the converter thyristors' control angle and in the feed network voltage, all of which can be observed when compensating for disturbances of powerful output and energy, the use of a linear energy storage and power system model produces considerable errors. This is why the appropriate control laws need to be used to regulate the energy storage unit. In order to regulate a non-linear object such as an IN, several control systems have been found acceptable, some of which are systems with deep feedback or which use non-linear elements and elements with alternating transfer constants which compensate for the basic linearities of the unit being controlled. Regulating systems which fine-tune the parameters are ill-suited for regulating a power system's transition processes.

Let us consider the basic non-linearities of the IN from the standpoint of control. When removing the external characteristics of the experimental IN, it was shown that the increase of the true (active) and reactive power of the IN relative to the converter thyristors' angle of control (α) depends non-linearly on signal (z) itself, and on the IN charge (z) or current (I_n) and on the voltage of the alternating current feed network (U). The relation of similar characteristics to the voltage frequency is negligible.

The differential equations which describe the change in the IN output depending on α, z and U can be shown as follows:

$$P_n^{(n)} = f(\alpha, z, U, P_n) + B(\alpha, z, U)\alpha,$$

where f and b are non-linear functions; α is the control angle for the converter's thyristors; $P_n^{(n)}$ is the leading derivative of the IN's active power. When regulating α in accordance with the law

$$\alpha = k\left[F(P_n, t) - P_n^{(n)}\right],$$ where $F(P_n, t)$ is the desired change P_n, i.e., when regulating according to the difference between the desired and measured values of the n derivative of P_n we obtain

$$P_n^{(n)} = \frac{b(\alpha, z, U)k}{1 + b(\alpha, z, U)k} F(P_n, t) + \frac{f(\alpha, z, U, P)}{1 + b(\alpha, z, U)k},$$

and that when $k \to \infty$ leads to the fact that where $P_{rasp} \geq P_n$, where P_{rasp} is the available power of the IN and $P_n^{(n)} \approx F(P_n, t)$ and does not depend on z and u. The advantages of this method of synthesis lie in the provision of the required dynamic and static characteristics for the IN in a wide range of changes in the electric power system's operating conditions and in the IN's parameters.

Let us examine a second method for compensating for non-linear power storage unit characteristics. Since the greatest interest is in using an IN to regulate true power in an electric power system, let us examine the compensation of an IN's non-linearities relative to the control angle for a converter's thyristors.

Since $P_n \approx U_n I_n \cos\alpha$, when alternating gain factor $k_n = \arccos(v/(U_n I_n))$ is introduced into the regulating circuit, this compensates the basic non-linearities of the energy storage unit for active (true) power relative to the controlling signal v.

The required gain, or transmission factor for the true power signal for the IN relative to control v can be realized in two blocks with an alternating gain factor of type

$$k_{n1} = 1/U_n, \quad k_{n2} = 1/I_n$$

and in the non-linear block which performs function arc cos.

The second method of compensating for the basic non-linearities of the IN is the simplest and most convenient to work out on analog computers. This is also the method used on an analog regulator with the IN operating within the power system.

Several regulating laws were used to regulate the IN, one of which takes the following form:

$$v = -k_{n}k_{n_2}k_1\left\{k_2\left[P_{lep}\left(k_3 - k_4\frac{1}{1+pT_2}\right)\left(\frac{pT_1}{1+pT_1}\right) + P_n k_5\frac{pT_3}{1+pT_3} + Q_{lep}k_6\frac{pT_4}{1+pT_4}\right] + k_7\left(P_{lep} - P_{lep}^{pred}\right)\right\} + (I_n - I_{ust})k_8\frac{1+pT_5}{1+pT_6},$$

$$\alpha = \arccos v + \alpha_0,$$

where $k_{n1}=1/U_n$, $k_{n2}=1/I_n$; k_5 and k_6 are constant control factors; T_1--T_6 are time constants; p is the Laplacian operator; $k_1=1$ where $I_n < I_n^{max}$, otherwise $k_1=0$; $k_2=1$ where $\Delta P_{lep} < \Delta P_{lep}^{pred}$, otherwise $k_2=0$, $k_3>0$, $k_4=0$ where the power transmission line switch is engaged, otherwise $k_3=0$, $k_4>0$; $k_6>0$ when $\alpha_{1\ 2} < \frac{\pi}{2}$, otherwise $k_6<0$; $k_7=0$ when $P_{lep} < P_{lep}^{pred}$, otherwise $k_7>0$; P_{lep} is the transfer of true (active) power along the power transmission line; P_{lep}^{pred}, and the limiting transfer of power along the power transmission line according to the conditions for static stability of the power transfer along the LEP [power transmission line]; ΔP_{lep} is the change in the power transfer along the power transmission line; P_{lep}^{1} is the derivative of P_{lep}; P_n is the true (active) power of the inductive storage unit on the alternating current side; I_n is the IN current; I_{ust} is the current unit of the IN which provides the maximal control range for the true (active) power; U_n is the acting value for the voltage on the thyristor converter from the alternating current direction; is the control angle for the converter thyristors; is the initial value for the thyristors' control angle.

The derivative of the transfer of true (active) power along the power transmission line is used to compensate for the high-frequency spectrum of the true (active) power disturbances along the power transmission lines. The low-frequency spectrum can be compensated in this instance by turbine regulators. The width of the compensated IN spectrum of disturbances depends on time constant T_1, which is selected based on the amplitude and duration of the calculated disturbances, the technological limitations on the transformer's operating conditions, the thyristor converter and the inductance coil, and can also depend on the high-speed response of the turbine regulators. The channel for derivative P_{lep} is put to work during power transfer disturbances which are higher than the locating derivative so that the systems can help each other during disturbances, can provide dynamic stability in the electric power system and can increase the power transferred along the power transmission lines to the power reserve for stability for irregular disturbances in power transfer P_{lep}. An inductive accumulator shield is introduced into

the regulator to protect it from overloads. It switches the control circuit off when the inductive accumulator current exceeds the maximum installed current. In the block diagaram, the shield is realized in the comparator unit and polar relay K3 (Fig 2). In order to make the power system statically and dynamically stable, a channel is introduced to control the limiting power transfer along the power transmission line.

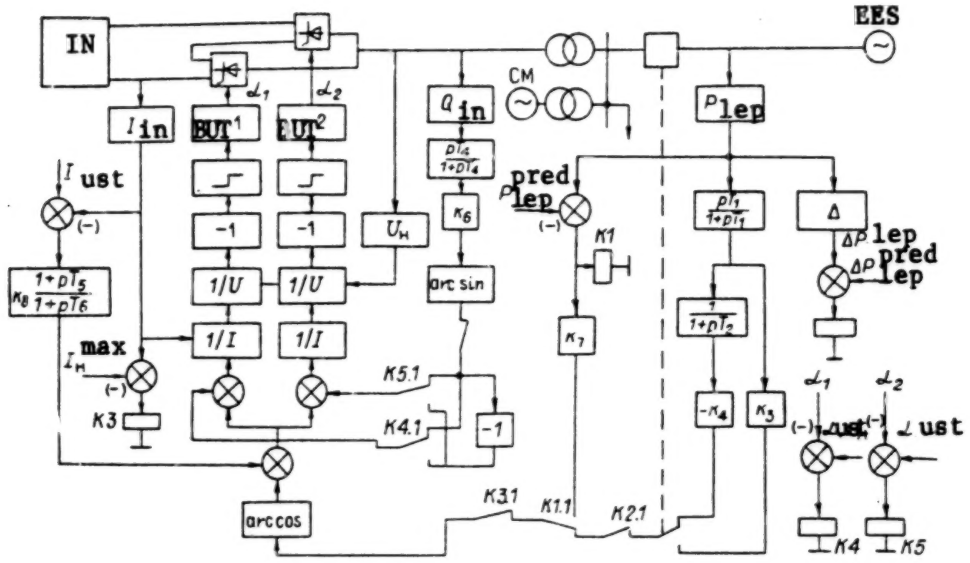

Figure 2. Block Diagram of IN Regulator

During the no-current condition of the automatic reclosing (APV), the signal of the derivative P_{lep} is introduced into the control law with an opposite sign to provide the requisite change in the frequency in the remaining portion of the power system to which the IN is connected. The low-frequency equalizer which blocks high-frequency noise in the control circuit when the electric power system is in non-symmetrical operation is switched on when the automatic reclosing at the IN connection point is in no-current condition. In order to ensure that the IN charge is of the required value, a control circuit has been introduced into the IN current, which is the secondary control circuit with relation to the circuit for the P_{lep} derivative.

In order to reduce the reactive power consumed by the IN and provide its required value, the IN is connected to the power system via the two converter thyristors. In order to control the IN's reactive power, the signal for derived reactive power, which is taken from a real differentiation link having the required constant of inertia, is fed in the two converter thyristors. Since with converter thyristor control angles equal to $\pi/2$, the IN reactive power feedback and the losses of stability in the control system, the reactive power control signal for the IN where $\alpha_{1,2} > \pi/2$ is inverted. Within the regulator are control action limitations on the converter thyristors' control angles which prevents losses of stability in the control circuit when more than a dual-rectifier stable operating condition arises. A block diagram of the

regulator is shown in Fig 2. The operational fitness of the regulator has been checked out in experiments with an experimental model of the IN working as part of a power system.

During the experiments several problems related to using the IN to provide stability and quality to the electric power system's processes were examined. Thus, while predominantly using synchro motors with BAPV [high-speed automatic reclosing] to provide the load center with dynamic stability, true (active) power equal to the pre-emergency power transfer through the power transmission lines is required during the high-speed automatic reclosing pause of the IN, thereby absorbing the surplus power of the switched-on synchronous machine (P_{sm}) (see Fig 3).

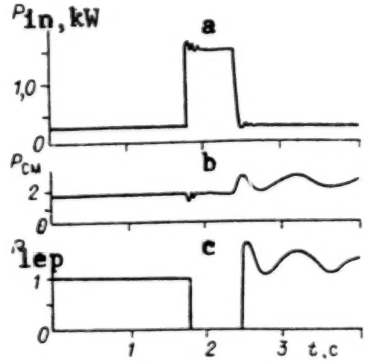

Figure 3. Pairing of disturbances in true (active) power by the inductive power storage unit during short-term disengagement of power transmission lines.
Key: a--change in true (active) power of the IN; b--change in true (active) power of synchronous machine in the generating center; c--change in true (active) power transfer along power transmission lines.

From the results of the experiment shown in Fig 3, we see that the law used to control the IN provides an IN-equipped electric power system with dynamic stability. Without using an IN in this experiment, the electric power system loses stability. The IN helps to compensate for disturbances in the active power sent along power transmission lines. Thus, from Fig 4 it is evident that during short-term load condition P_{nagr} the IN compensates for practically the entire load surge of active power into the electric power system.

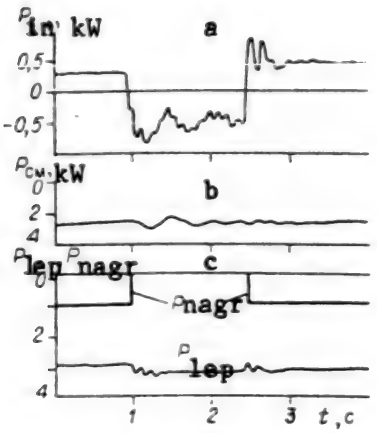

Figure 4. Countering disturbances of active power with an inductive power storage unit during radically changing load conditions in the generating center.
Key: a--change in active power of the IN; b--change in the active power of the synchronous machine in the generating center; c--change in the load output and the transfer of active power along power transmission lines.

The research conducted here allows us to conclude that using an IN can effectively compensate for high-frequency spectrum active power disturbances, can provide the power system with dynamic stability and can suppress synchronous machine rotor oscillations.

Siberian Scientific-Research Institute of Power Engineering, Novosibirsk

Submitted to editorial board on 4 March 1988

BIBLIOGRAPHY

1. S. A. Sovalov: "Rezhimy Yedinoy energosistemy" [Unified Power System Operating Conditions].--Moscow: Energoatomizdat, 1983.

2. "Avtomaticheskoye regulirovaniye i upravleniye v energosistemakh" [Automatic Regulation and Control in Power Systems].--Moscow: Energoatomizdat, 1983.

3. Patent No 618819 (USSR). "Sposob sokhraneniya ustoychivosti pri avariynom defitsite aktivnoy moshchnosti" [Method of Maintaining Stability During an Emergency Shortage of Active Power]/ Ukrainian Division of Energosetproyekt [All-Union State Planning, Surveying and Scientific Research Institute of Power Systems and Electric Power Networks]; G. V. Kolonskiy--Application 25 October 1976, No 2413106. Published 02 August 1978, MKI N 02 3/24.

4. I. E. Glebov, A. Ya. Popov and A. G. Ter-Gazaryan: "Optimizatsiya rezhima raboty energeticheskogo nakopitelya v energosisteme" [Optimizing the Operation of the Power Storage Unit in a Power System] // "Puti

ekonomii i povysheniya effektivnosti ispol:zovaniya elektricheskoy energii v sistemakh elektrosnabzheniya promyshlennosti i transporta" [Methods of Economizing and Improving the Effectiveness of Using Electric Power in Industrial and Transport Power Supply Systems].--Kazan, 1984.

5. M. Masuda, T. Shintomi and K. A. O. Kaminosono: Power System Stabilization by Superconducting Magnetic Energy Storage. Experiment Using Power System Model // Proceedings of the 9th International Cryogenic Engineering Conference, Kobe, 11-14 May, 1982.--Guilford.--1982.

6. H. J. Boenig and J. F. Hauer: Commissioning Tests of the Bonneville Power Administration 30 MJ Superconducting Magnetic Energy Unit // IEEE Trans.--1985--Vol. PAS-104, N 2.

7. N. L. Novikov, V. K. Khalevin and V. M. Zyryanov: "Povysheniye rezhimnoy nadezhnosti energoobyedineniy so slabymi mezhsistemnymi svyazami s pomoshchyu upravlyayemykh induktivnykh nakopiteley" [Using Controlling Inductive Storage Units to Improve the Operating Reliability of Power Associations Having Weak Inter-System Links] // "Nauchno-technicheskiye i tekhnologicheskiye voprosy sozdaniya sverkhprovodnikovogo elektroenergeticheskogo oborudovaniya" [Scientific-Technical and Technological Problems of Developing Superconducting Electric Power Equipment]: Thesis Report. All-Union Scientific-Technical Conference.--Moscow, 1984.—Vol 1.

UDC 621.436

On the Indicators for High-Speed Carbureted Engines with Increased Exhaust Back-Pressure

18610545a Moscow IZVESTIYA VYSSHIKH UCHEBNYKH ZAVEDENIY: MASHINOTROYENIYE in Russian No 3, Mar 89 pp 36-39

[Article by Director of Technical Sciences, Professor B. S. Stefanovskiy, Candidate of Technical Sciences Yu. A. Grishin and A. T. Reppikh, post-graduate student: "Indicators for High-Speed Carbureted Engines with Increased Exhaust Back Pressure"]

[Text] (Italics) Based on data obtained while testing an engine, this article examines the influence of exhaust back pressure on engine power and economy. It also evaluates the indicators for a turbocharged engine operating with the same level of back pressure and analyzes the question of the feasibility of turbocomponding.

There is great practical value in looking into the effect of increased exhaust system back pressure on the indicators for high-speed carbureted (gasoline-powered) engines. The results allow us, first of all, to evaluate the potentialities of these or other mufflers and devices which neutralize the toxic components of VG [exhaust gases], and second, considering that an extremely significant proportion of thermal and mechanical energy [1] is carried away with the exhaust gases from carbureted engines, make it possible to evaluate the possibility of using these or other devices which utilize exhaust gas energy, particularly power turbines (the turbocompound system).

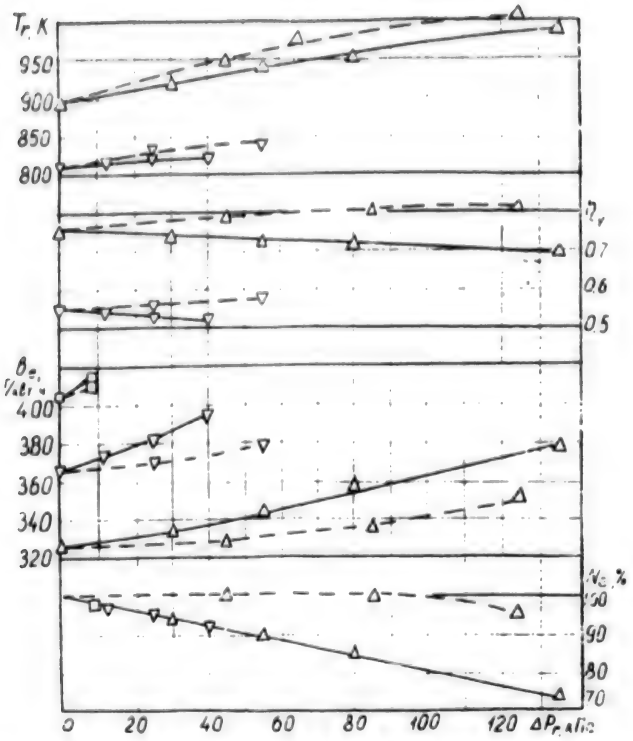

Figure 1. The effect of exhaust back pressure on engine indicators when α= 0.9; the solid line represents the effect without compensation for power losses; the broken line represents the effect with compensation; v_a, in kg/hour; □ =60; ▽=90; △=120

Figure 1 shows the relationship of the indicators for a high-speed carbureted engine to the amount of resistance Δp_r in the exhaust system generated by restricting the exhaust manifold. Rotational speeds and loads were tested which corresponded to a motor vehicle traveling at speeds v_a=60, 90 and 120 km/hour on rich (α=0.9 and) and lean (α=1.1) fuel mixtures. In compliance with GOST 14846—81, all engine parameters were measured with the engine operating uncompensated for power losses caused by increased back pressure and with power compensated to the initial level (without back pressure) by opening the carburetor butterfly valve.

From Fig 1 it is evident that in the first instance (without compensation), increasing the back pressure lowers the power equally at all traveling speeds equally. Where Δp_r is equal to 100 kPa, the power losses amounted to approximately 20 percent, while opening the carburetor butterfly valve to a corresponding degree compensated for these losses almost completely.

Increased exhaust back pressure and power losses negatively affected the engine's economy. Thus, at a traveling speed of v_a=90 km/hour, exhaust back pressure of 40 kPa (roughly corresponding to the resistance generated by a normal muffler) improved the fuel consumption rate by roughly 30 g/kW · hour, or almost 10 percent. This lowers the coefficient of charge. Inasmuch as engine economy fell off considerably more than

power, this indicates not only a worsened gas exchange, but also a combustion process deviating from optimal.

From the practical standpoint it is significant that when power losses were compensated, engine power fell off far less: for example at the same regime (90 km/hour) the specific effective fuel consumption rate increased by only 8-10 g/kW · hour. This is because using this control method, the coefficient of charge did not decrease with increased back pressure, but increased. Naturally, as this occurred, the gas exchange improved, pump losses decreased, and the negative effect of increased back pressure was compensated to a great extent.

Examining the operation of a carbureted engine with regard to using the energy from exhaust gases, it is easy to be persuaded (Fig 1), that increasing exhaust back pressure does not lower exhaust gas temperature T_r. Thus, the gases have a considerable reserve, not only of mechanical, but of thermal energy, which can be used effectively to markedly increase the engine's power and to improve its economy.

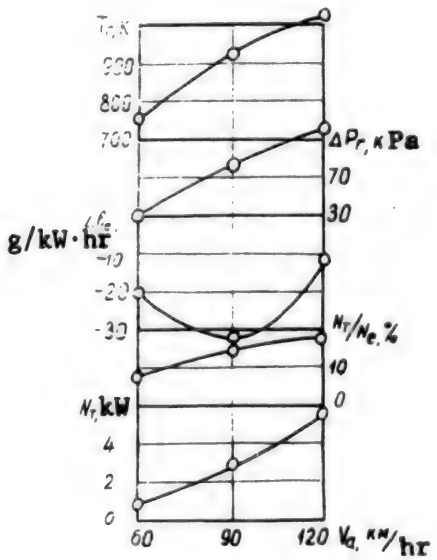

Figure 2. Indicators of effectiveness of using exhaust gas energy in a turbine when η_t=0.7.

In order to evaluate the degree to which these indicators can be improved, they were calculated for the above-mentioned vehicle traveling speeds assuming that the gases with the parameters shown in Fig 2 will be used in the turboreducer unit, which has an efficiency factor of η_t= 0.7 and which gives up its power to the engine's crankshaft. The results of the calculations are shown in Fig 2. These results establish that the turbine's power accounts for a tangible share (10-20 percent) of the engine's power at all regimes. According to this, the specific effective fuel consumption rate of the turbo-equipped engine falls off significantly (by 10-30 g/kW · hr).

The results obtained allow the idea of compounding high-speed carbureted engines to be given a positive evaluation. However, there arises the question of the degree of feasibility of this idea.

The point is that gas-turbine superchargers for these engines have extremely high rotational speeds--150,000 min^{-1} and even higher [2]. If the power turbine is to be equally high-speed, then when the crankshaft is rotating at 5,000-6,000 min^{-1}, cumbersome and uneconomical reduction gearing must be mounted between them. Mass production and use of these reducers will hardly be profitable. However real opportunities exist for developing much lower-speed power turbines.

The first of these opportunities consists in changing over from reaction turbines to impulse turbines with two or three stepped speeds. We know [3] that the optimal ratio of circumferential velocity u for these turbines to rate c_1, at which the gases escape from the nozzles, is considerably reduced. With two or three stepped speeds, the turbine's rotational speed can be lowered to 10,000-20,000 min^{-1}, and the gear ratio for the reduction gear in this case would be all of 2-4, which is completely acceptable and technically easily realizable. As for making the turbine itself more complicated, this problem can be reduced to a minimum, for example, by using the Kinast design, whereby the gas interacts repeatedly with the same ring of turbine blades. The rotational speed can by lowered by using a vortex turbine [4] and correspondingly refining the flow-through parts, which provides a high degree of efficiency. In these turbines the gas also interacts repeatedly with the blade rim and moves in a spiral through the ring channel from intake to discharge (Fig 3).

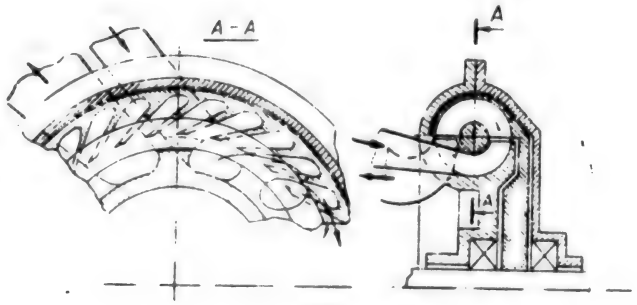

Figure 3. Diagram of a vortex turbine

These turbines are reliable and durable and the blades act as excellent heat exchangers, since there is a considerable amount of rotor contact surface compared to the blades on other types of turbines. An important advantage, particularly as applied to internal combustion engines, is its low sensitivity to exhaust gas impulses and its slow-speed working range. The rotational speed of vortex turbine rotors is slower by an order of 1-2 than that of axial and radial turbines [5], which allows them to be used in turbocharged engines without using complicated step-down gearing. The simple design of these turbines allows them to be used on passenger car engines.

The small loads used to test the rotor parts and primarily the working blades, which derive from the low rotational speed, is a product of their reliable operation when they are manufactured from ceramic and composite materials. This is especially urgent for use in carbureted engines and prospective adiabatic internal combustion engines with high-temperature exhaust gases.

BIBLIOGRAPHY

1. N. K. Shokotov, S. M. Shakhidula and A. P. Marchenko: "Otsenka effektivnosti vtorichnogo ispolzovaniya teploty otrabotavshikh gazov karbyuratornogo dvigatelya" [Evaluation of the Efficiency of Secondary Utilization of Heat from Spent Carbureted Engine Gases]// Dvigateli vnutrennego sgoraniya. Kharkov. 1986. pp 3-8.

2. Turbochargers: A signal success // INDUSTRIAL LUBRICATING AND TRIBOLOGY, No 1, 1987. pp 10-11.

3. B. S. Stechkin, P. K. Kazandzhan, A. P. Alekseyev et al: "Teoriya reaktivnykh dvigateley. Lopatochnyye mashiny" [Theory of Reactive Engines. Turbomachines] / Moscow: Oborongiz, 1956.--543 pp.

4. O. V. Baykov: "Vikhrevyye gidravlicheskiye turbiny" [Hydraulic Vortex Turbines] // IZVESTIYA VUZov. MASHINOSTROYENIYE.--No 9, 1974--pp 72-76.

5. V. N. Khmara, V. N. Sergeyev and S. M. Vaneyev: "Rabota vikhrevoy mashiny v rezhime pnevmoprivoda" [The Operation of Pneumatically Driven Turbomachines]//IZVESTIYA VUZov. MASHINOSTROYENIYE. No 9, 1985. pp 59-62.

Article submitted 1 July 1988

621.891

Anti-Wear Diesel Fuel Additives Investigated

18610545b Moscow IZVESTIYA VYSSHIKH UCHEBNYKH ZAVEDENIY: MASHINOSTROYENIYE in Russian No 3, Mar 89 pp 44-47

[Article V. Ye. Gorbanevskiy and T. V. Ternovaya, candidates of technical sciences, and Doctor of Technical Sciences V. T. Maslov: "The Wear-Resistant Effect of Certain Substances in Diesel Fuel During Long-Term Operation of Steel Friction Pairs". First two paragraphs in italics.]

[Text] This article examines the positive effect of the substance MD, which is used as an additive to DL [summer diesel] fuel to promote wear-resistance for steel friction pairs.

The experiments described here were conducted on an MT-5 friction machine which moved one of the samples reciprocally under a constant 40 MPa load and at an average relative-motion speed of 0.19 m/sec for 140 hours. The experiments were conducted in pure diesel fuel and in the same fuel with MD additive accounting for 0.5 percent by mass.

The experiments ascertained the self-oscillating character of the change in the concentration of the substances which were introduced and which formed while the friction pairs were operating. Moreover, the friction surfaces of these substances displayed no noticeable fracturing.

One of the primary tasks involves substantially prolonging the durability of various friction pairs which operate in fuels with poor tribotechnical properties. There are well-known manufacturing approaches for preventive treatment of the surfaces of the parts making up these friction pairs. These approaches were meant to improve their wear- and corrosion-resistance, but either fall short of their goal, or cause secondary negative effects [1]. At the same time, introducing anti-wear, anti-score, anti-corrosion and other additives with a broad range of effects into friction assemblies which operate in oils and lubricants is an effective and economically advantageous way to to improve the wear-resistance of friction assemblies which work in these mediums. This method of reducing the wear on pairs which function in fuels has been little studied due to the practical absence of substances capable of working effectively in fuels.

We studied the behavior of MD in sliding friction assemblies designed to imitate the work of steel piston pairs in diesel fuel equipment under a fairly heavy load and relatively long-term operation. The results of this study are given below.

As an experimental check has shown, it is not so much the type of contact as the nature of the relative movement of the parts making up the friction pairs which most influences the operational fitness of friction pairs [2]. This is why, when the work of the most crucial steel friction pairs in diesel fuel-handling equipment--i.e. the precision plunger pairs--is modeled on a friction machine, we need to ensure that they move in their characteristic reciprocating motion. This relative motion of the models was duplicated on an MT-5 friction machine, which was used in the research, but with the moving (2) and stationary (1) metal samples moving in close contact. The experiments were conducted at a constant load of 40 MPa and with sample 2 moving at an average speed of 0.19 m/sec. Here, the stationary sample had less friction surface (4 x 25 mm) and the moveable sample has more (40 x 25 mm). Both samples were manufactured of ShKh15 steel, hardened to RC 60÷65, with a friction surface roughness in the direction of friction of 0.6 mcm for the stationary model and 0.10÷0.12 for the moveable model; the friction surface roughness across the direction of motion was 0.7 mcm for the stationary model and 0.90÷1.15 mcm for the moveable model.

Purified MD with no more than 0.1 percent impurities was introduced at 0.5 percent by mass into type DL summer diesel fuel.

Some 150 milliliters of fuel were poured into each chamber of the multiposition MT-5 friction machine. The entire experiment lasted 140 hours. A portion (3 ml) of fuel was drawn off into a test tube every 7 hours for subsequent chemical analysis. The rate of linear wear for each model was determined at 7-hour intervals. For this, the models were removed from the friction machine, washed in gasoline and weighed on analytical scales with an accuracy of up to 0.2 mg. The rate of wear on each of them was then determined via a calculation in accordance with method [3].

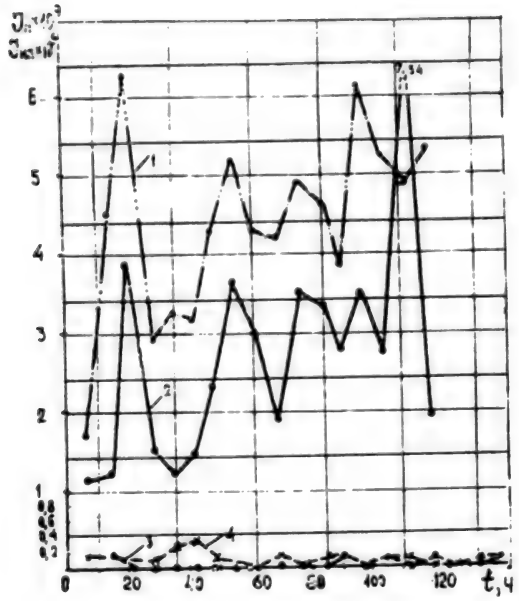

Figure 1. The relationship of the rate of linear wear on steel friction pair models to the duration of their operation: 1--stationary model in diesel fuel; 2--moveable model in diesel fuel; 3--stationary model in diesel fuel with MD additive; 4--moveable model in diesel fuel with MD additive

Figure 1 shows the graphic dependence of the rate of linear wear on the duration of the work of the friction pairs. Curves 1 and 2 represent the wear on the stationary and moveable models, respectively, in pure DL fuel, and are typical for the rate of wear of steel pairs in fuel. With the introduction of the MD additive it can be observed that the same pairs work almost wear-free for the duration of the entire experiment (curves 3 and 4). Several of the lowest points (located, with regard to wear, much lower than similar points where the model is working in pure fuel) appear as the result of random influences in the selection of pairs for weighing the models and their subsequent assembly, for example, because of microfractures of the relative position of the models, etc.

The rate of wear for both models when working in clean fuel fluctuates roughly around the mean value for each: $4.39 \cdot 10^{-9}$ for the stationary models and $2.73 \cdot 10^{-9}$ for the moveable models. With the addition of MD, the rate of wear on both models also has a tendency to fluctuate from stage to stage. But here, the fluctuation occurs in the vicinity of zero values fixed for these and the other models on 5-13 stages out of 20. Taking into account the above-mentioned low points, the average rate of wear in the presence of MD came to: $0.62 \cdot 10^{-9}$, which is less by a factor of 71 than in pure DL fuel (for the stationary models), and $0.266 \cdot 10^{-9}$, which is less by a factor of 10 than in pure fuel (for the moveable models).

When the models are operating in clean fuel, wear on the working surfaces can be observed visually at the initial stages. When MD is used, the condition of the surfaces remains noticeably unchanged throughout the experiment. Only a film of the substance itself appeared on the surfaces, tinting them a faint violet.

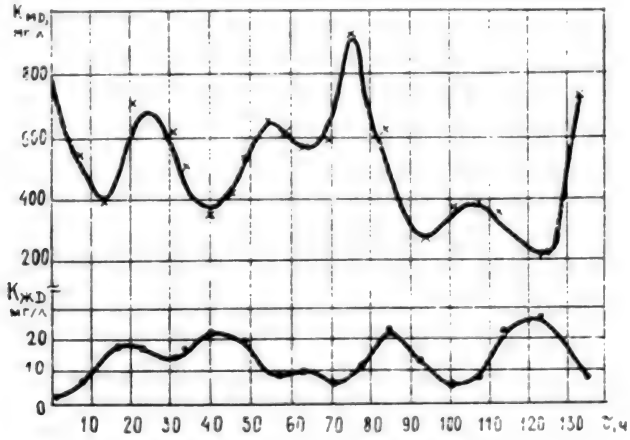

Figure 2. Change in the concentrations of introduced MD (K_{md}) substance and the iron-bearing substances (K_{zhd}) depending on the duration of the working period (according to the results of atom-absorption ultimate analysis of the fuel).

The results of a chemical analysis of fuel plus MD were obtained via standard methods and are shown in Fig 2, which shows that in the first ~15 hours of operation, the MD concentration diminished and the concentration of solute iron (samples of the fuel were centrifuged to precipitate the finely-dispersed particles of worn metal) increased. During the succeeding 15÷20 hours, the opposite was observed: the MD concentration increased and the iron concentration diminished.

Thus, it was established that the changes in the concentrations of the introduced substances and those which formed during the operation of the friction pairs were self-oscillating, and that with time there were no noticeable fractures of the surfaces and substances. This relationship was completely reproduced in two identical experiments: all the peaks practically coincided. The amplitudes of the change in concentrations of the substances are different, but they repeatedly exceed the sensitivity and accuracy of the measurements (the sensitivity of the analysis for iron comes to 0.1 mg/liter and for MD was 10 mg/liter, and the accuracy of the determination was 5...10 percent of the relative). The oscillating nature of the change in the concentration of the substances unconditionally reflects the same character of molecular processes which were not studied, but which are capable of reducing the wear on steel friction pairs in diesel fuel.

BIBLIOGRAPHY

1. V. Ye. Gorbanevskiy and V. G. Lapteva: "Vybor metodov povysheniya isnosostoykosti par treniya, izgotovlennykh is stali tipa ShKh15 [A Selection of Methods for Improving the Wear-Resistance of Friction Pairs of Type ShKh15 Steel]. TRENIYE I IZNOS, No 1, Vol 9, 1988 pp 43-51.

2. A. Ya. Shepel, V. Il Lyulko, V. Ye. Gorbanevskiy et al: "Protivozadirnyye i protivoiznosnyye svoystva dizelnykh topliv i benzinov" [Score- and Wear-Resistant Properties of Diesel Fuels and Gasolines] // DVIGATELESTROYENIYE, No 2, 1982 pp 45-47.

3. Ye. N. Dokuchayeva, V. G. Lapteva and V. F. Kaplina: "Iznosostoykost konstruktsionnykh materialov" [Wear-Resistance of Structural Materials] / Spravochnyye dannye po rezultatam laboratornykh ispytaniy.-- Moscow: izdatelstvo NIITSKhM. 1977. 163 pp.

Article submitted on 22 February 1988

UDC 658.527.011.56:621.757.06-52

Unique Satellite Assembly Line Developed

18610546b Moscow MASHINOSTROITEL in Russian No 5, May 89 p 21

[Article by V. B. Babin, L. I. Nikonovich, Ye. N. Kovalev and K. I. Degtyarev: "A Satellite Assembly Line With a Non-Synchronized Operating Pace"]

[Text] The Gomel Production Design and Experimental Institute has developed an automated satellite assembly line (a. s. 1316794 and 1305101), which operates at a non-synchronized pace for the Liyepaysel-mash [Liyepaya Agricultural Machinery] Plant. The line assembles and tests telescoping cylinders.

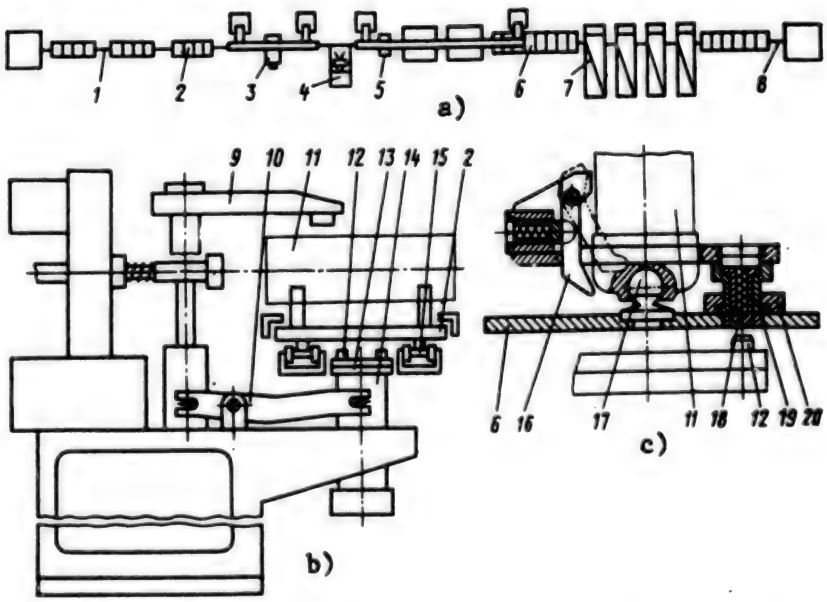

The assembly line consists of two vertically closed transport systems 1 and 8. Transport system 1 (Figure a) with satellite fixtures 2 (22 pieces) links the sleeve-pressing unit to the thread-cutting lathe in the production sequence. Transport system 8 with its satellite fixtures 6 (18 pieces) in turn uses the working fluid of the assembled hydraulic cylinders to link the test stands 7. Automatic manipulator 5, which transfers the assembled products from transport system 1 to transport system 8, is also part of the assembly line.

The satellite fixtures of each transport system are arranged on drive chains. The workpieces are secured to the satellites and clamped down with mechanized assembly equipment and stands in preparation for the operations and tests to be performed on them right at the production stations. The satellites move on the working conveyers at 0.13 m/s, and along the return conveyers at 0.2 m/s.

The telescoping hydraulic cylinders are assembled on satellite fixtures 2. Satellite fixture 2 is set in the thread-cutting assembly position and workpiece 11 is clamped (Figure b) in one pass of the unified power drive of hoist 14. The satellite fixture, which is carried along by chain drives 15, travels to the assembly area stop. As this occurs, a signal is sent to activate the drive unit and the chain carriers slide past beneath the stopped satellite fixture. The power cylinder moves plate 13 vertically upward, which puts lever system 10 into operation, and moves clamp 9 downward. As grip pins 12 enter the corresponding holes in the satellite and it is fixed, the workpiece is clamped. After the manufacturing operation has been performed, the satellite fixture is released and the workpiece is unclamped in reverse order.

Completely assembled hydraulic cylinder 11 is repositioned onto transport system 8 by automatic manipulator 5, which sends it on to test stands 7.

The hydraulic cylinder is mounted on a hinged support (Figure c) on satellite fixture 6 and held there by levers 16 in the vertical position (i.e. in the position the hydraulic cylinder will occupy in the machine). When the satellite fixtures arrive at the station at which the hydraulic cylinder is fixed in the testing position, fixing pins 12 push plungers 18 out of the holes in the satellite base, which allows round protrusions 19 to move along the rounded grooves in bars 20. This rotates the workpiece being tested around the axis which passes through the center of the rounded protrusions and the hinged support. This fully imitates the hydraulic cylinder's operating conditions. When all the tests have been completed, transport system 8 (Fig a) moves the hydraulic cylinders to the unloading position.

The line can assemble 42 items per hour and is served by 5 workers. The line's dimensions are 33,300 x 2,800 x 1,650 mm.

The inclusion of test stands in the assembly line greatly enhances its manufacturing capabilities and labor productivity by performing complete tests of the assembled hydraulic cylinders directly on the assembly line without having to take them off the satellite fixtures and by fixing them while simultaneously securing the workpieces at the assembly points. The absence of clamping elements on the satellite fixtures greatly simplifies their design and reduces the amount of metal in each satellite unit as well as the amount of metal in the entire line. In addition, the use of the line frees five fitter-assemblers.

UDC 621.865.8-229.29

Manipulator Gripper Discussed

18610546c Moscow MASHINOSTROITEL in Russian No 5, May 89 pp 21-22

[Article by V. D. Darovskikh: "Manipulator Gripper"]

[Text] This gripper (a.s. 1248794), which is designed for a manipulating mechanism used to robotize the application of galvanized coatings, has greater manufacturing capabilities and can automatically change its parameters when the size of the workpieces being gripped is changed.

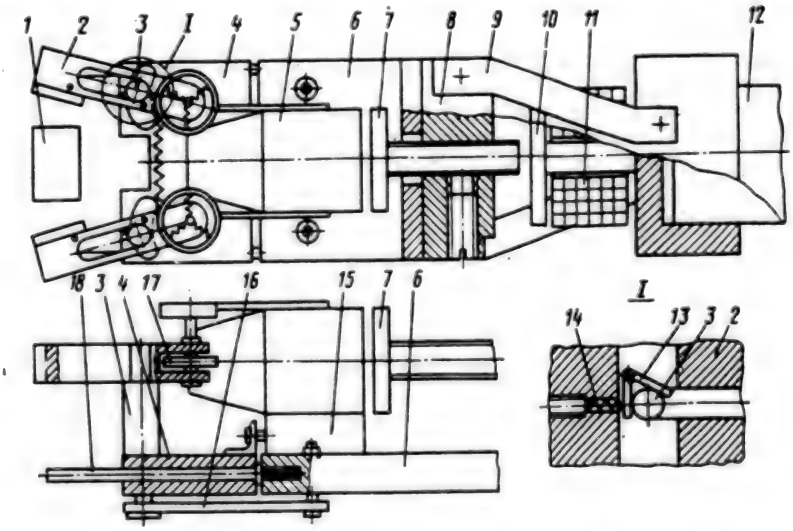

The device is based on housing 6 and a gripper made of two spring-loaded levers 2 with rollers 17 and drives 5 and 15 for the gripper and for linear movements of the platform. The levers are mounted by joints on movable platform 4. There is also a vibrator made of electromagnet 11. The gripper is fitted to manipulator 12. Both drives and the electromagnet are disengaged when in the initial position. Spring-loaded levers 2 are separated and the faces of yoke 8 and core 10, when acted upon by springs 9, form a gap between themselves. There is also a gap between control screw 7 and the core. Gripper drive 5 is engaged, rotating levers 2 relative to pins 3 and gripping workpiece 1. Electromagnet 11, which is fed pulsating voltage, is then switched on. When the electromagnet is activated yoke 8, which is joined to housing 6, is pulled toward core 10, which compresses spring 9. When the electromag-

net is switched off, the yoke is returned to initial position by the same springs. The springs are mounted at an angle to the axis of the electromagnet and give the device forward-rotating oscillations necessary to grip workpieces with complex shapes. Screw 7 controls the amplitude of the oscillations. The oscillations stop when the voltage is turned off. Drive 5 is switched off when the manufacturing process is completed, and levers 2 release the workpiece.

When the size of the workpiece to be gripped is changed, drive 15 for platform 4 is engaged. The latter is moved linearly along guides 18, which are fitted to housing 6 and which force pins 3 to move along the longitudinal grooves in levers 2. As this occurs, the pin rotates clamp 13 around its axis and the clamp is set by spring 14 into the groove in the platform so that its free end does not protrude into the lever's longitudinal groove. The pin self-aligns with the platform groove thanks to the rotation of pullrod 16 and its linear movement together with the pin around the axis connecting the pullrod with housing 6. A change in the position of the pin's axis relative to the lever's longitudinal groove changes the coefficient of force of the levers and the extent of the working movements of their ends. And after they are reset, the final positions of the levers' gripping jaws are parallel to their initial position. The pin is fixed to lever 2 by clamp 13 as it rotates around its own axis when acted upon by the spring-loaded end of the clamp of the linearly-moving pin. The pin is disengaged when the working load developed by the platform drive exceeds that of the grip drive, which stems from the way they were set up beforehand.

The automatic change of the gripper's parameters shortens the set-up time for the operation, and rules out the participation of an operator in the readjustment process.

UDC 621.793.002.3-419
621.793.7:621.7.044.2

Antifriction Detonation Coatings

18610546d Moscow MASHINOSTROITEL in Russian No 5, May 89 pp 33-34

[Article by V. Kh. Kadyrov and V. V. Shchepetov, candidates of technical sciences: "Antifriction Detonation Coatings"]

[Text] The detonation-gas method is a state-of-the-art method for applying high-quality protective coatings. The widescale introduction of detonation coatings has been hindered by the dearth of reliable data on the tribotechnical characteristics of sprayed coatings and the areas where they are used with optimal technical and economic effect.

The properties of these coatings, which work under conditions of friction, depend on the operating requirements and vary widely depending on specific conditions. It has been found difficult to develop a universal anti-friction coating suitable for use in a variety of operating conditions. At present, a whole series of tribotechnical tests should be conducted relative to developing the technical processes involved in detonation spray-coating for the purpose of determining the friction pairs.

The present work presents the experimental results of research into the anti-friction properties of detonation composition coverings sprayed via nickel-chrome alloy powder containing dispersed molybdenum disulfide. The physico-chemical properties of molybdenum have been fairly well studied. Molybdenum disulfide is usually used in powder form, rubbed into the working surface, applied as a film-type binder, or deeply imprinted into surfaces when lubricating via the rotaprint method. Baked materials making up metallic dies with solid lubricants spread on them--usually graphite or molybdenum disulfide--are being widely used in friction assemblies.

A method was worked out for producing composition powders composed of nickel-chrome with molybdenum disulfide for use in detonation spraying of coatings. The particles of solid lubricant were no larger than 5 mcm. The molybdenum disulfide was wet-mixed with the nickel-chrome alloy powder. Experiments determined the optimal content of molybdenum disulfide in the multi-component powder making up the composition based on nickel-chrome alloyed with boron and aluminum. With less-than-optimal values, the coating failed to self-lubricate. Large amounts

of molybdenum disulfide caused the coating to disintegrate the coating and greatly reduced its bearing capability.

During the investigation of the anti-friction properties of detonation coatings containing dispersed molybdenum disulfide (Ni--Cr--Al--B--MoS_2), tests were conducted using the face scheme for contact in an air medium while making changes in the slip speed from 0.1 to 1 meter per second at a constant load of 1.5 MPa. The test results are given below:

Slip speed, m/s.....	0.1	0.2	0.4	0.6	0.8	1.0
Reported wear, mcm/cm^2.....	0.3	0.2	0.2	0.2	0.2	0.2
Coefficient of friction...	0.15	0.10	0.08	0.06	0.06	0.06

Increasing the slip speed in spite of the increased temperature in the friction zone lowers the friction coefficient and causes wear on the coatings under discussion. Across the entire range of slip speeds the coefficient of friction falls within 0.06...0.15. Thus, the presence of molybdenum disulfide in the contact zone greatly increases the anti-friction characteristics of detonation coatings working under conditions of friction.

The results of the experiments show that introducing dispersed molybdenum disulfide as a structural component of a nickel-chrome alloy composition coating provides an effective lubricant for the contacting surfaces under friction. The presence of a separating solid-lubricant film provides excellent anti-friction characteristics for the composite coatings under discussion and shows promise for their widescale use in various sectors of the machine-building industry.

UDC 621.9.02.002.3:666.3
620.17:666.3

Oxycarbide Ceramic Tool Reliability Discussed

18610546e Moscow MASHINOSTROITEL in Russian No 5, May 89 p 34

[Article by Yu. G. Kabaldin, doctor of technical sciences, B. Ya. Mokritskiy, V. N. Anikin, candidates of technical sciences and O. B. Kovalev: "Reliability of Oxide-Carbide Ceramic Tools"]

[Text] Oxide-carbide ceramic tools increase machining productivity and are capable of high cutting speeds. However, the spalling and chipping of oxide-carbide ceramic cutting blades lessen the stability of their cutting properties. Study of the physical nature of breakdowns of oxide-carbide ceramic tools has made it possible to determine ways of making them more reliable when used in flexible manufacturing systems.

The evaluative index K_{1s} attests to the fact that the crack resistance of domestically produced oxycarbide ceramics, other than TsM332 and V3 grades are equal in quality to the foreign ceramic Vidalox:

Ceramic grade	TsM332	V3	VOK60	VOK63	VOK71	Vidalox
K_{1s} MPa m	0.95	1.37	4.2	4.27	4.38	4.20

The weak link in the ceramic structure, which can be represented as a continuous oxide framework, is the Griffiths crack. A calculation of its critical size shows that it does not exceed 100 mcm.

Oxide-carbide ceramic is a heterogeneous tool material. The difference in the coefficients of thermal expansion of the structural components causes high density in the dislocations in the inter-granule boundaries of ($\rho \approx 10^{10}$ cm^{-2}), which may be why considerable internal stresses are generated.

Using electronic microfractography of fractures when a VOK60 oxide-carbide cutting blade is spalling, it has been established that areas of spaces have been observed spalling from the interfaces. Facets have been seen spalling from a chip of large aluminum oxide granules. Intergranule breakage in the area of small aluminum oxide and titanium carbide granules has also been seen. The formation of secondary microfractures accelerates the development of the main crack, causing the cutting blade to spall.

In order to study the effect of the internal stresses of oxide-carbide ceramics on resistance to brittle failure, vacuum annealing was performed where T=873...1,273 K. Research into the cyclical strength of annealed ceramics showed that the optimal machining regime is annealing where T=1,073 K for a period of 2 hours. The number of loading cycles until spalling of the cutting blades occurs increased 2-3-fold.

The aggregation of dislocations on the boundaries of the granules blocks the transmission of deformation from granule to granule. As a result, loading the boundaries of the granules localizes the dislocation, and thus concentrating the stresses facilitates the generation of microfractures. The possibility of the rapid spread of deformations depends on the structural heterogeneity of the oxide-carbide ceramic material and its internal defects.

Electronic microscopy of thin foil shows that after oxide-carbide ceramics are baked, a substructural mechanism is realized within them which strengthens the aluminum oxide and titanium carbide grains. Titanium carbides cause dispersed hardening of the matrix. Granules appear with a fragmented dislocation structure of ($\rho \approx 10^{12}$ cm^{-2}). This gives the ceramic material a high degree of wear resistance during continuous high-speed cutting.

Electronic investigations affirm that at high machining speeds the wear on oxide-carbide ceramics is plastic in character and is accompanied by a softening of the inter-granule boundaries and the formation of microfissures. This type of cutting blade rupturing happens to V3, VOK60 and VOK71 ceramics during lathe work on heat-treated steels.

Production tests of the fitness for work of V3, VOK60 and VOK63 oxide-carbide ceramic disks were conducted at the Amurlitmash plant (in the city of Komsomolsk-na-Amure). Cheek-pieces made of 40X steel with a hardness of 42...45 HRC were machined on a radial boring machine. The cutting conditions were: v=2.4 m/s, s=0.23 mm/rev; and t=0.5...2.5 mm.

The results of the tests of the plates tested to the point at which the cutting blade spalled are given in the table:

Material	Fitness for work, hours	
	during rough machining	during finish machining
VOK60	14	13
VOK60 with vacuum annealing	19	23
VOK60 with vacuum annealing and subsequent coating with a layer of zircon and then with a layer of zircon nitride	35	37
VOK60 with vacuum annealing and subsequent coating with a layer of niobium and then with a layer of zircon nitride	31	35

A statistical analysis of the production tests showed that vacuum annealing of oxide-carbide ceramics helps reduce standard deviation $\hat{\sigma}$ and coefficient of variation ν.

The economic effect of introducing oxide-carbide ceramics amounts to R20,000 per annum.

UDC 621.9.048.4.02:621.3.035.2
621.922.34.025.12

Diamond Wheel Cutting of Non-Ferrous Metals and Alloys Discussed

18610546f Moscow MASHINOSTROITEL in Russian No 5, May 89 pp 35-36

[Article by B. V. Morozov, candidate of technical sciences, and A. M. Senichev: "Cutting Non-Ferrous Metals and Alloys with Diamond Cutting Wheels"]

[Text] The Tula Polytechnical Institute has developed a method of cutting non-ferrous metals and alloys with diamond cutting wheels in a metallic bond. Essentially, this method consists of maintaining the cutting ability of the wheel's working surface during machining by electroerosion (or electric discharge) fracturing of adhered chips of machined material and wheel bond.

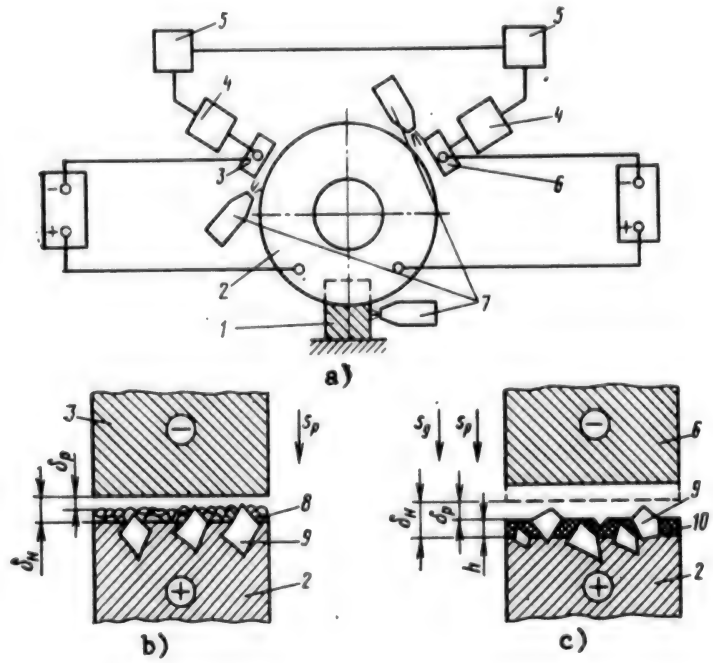

hen cutting workpiece 1 (Fig a) with cutting wheel 2, in order to maintain its cutting ability during the machining process, tool electrodes 3 and 6 constantly true the cutting wheel surface. The electrodes and the cutting wheel are connected to the direct current power

terminals. There are gaps between the tool electrodes and the working surface of the cutting wheel. The gaps are regulated by controlling transducers 5, which keep the gaps constant during the operating process via drives 4, which provide radial tracking s_r for the tool electrodes on the cutting wheel. Tool electrodes 3 and 6 perform a variety of functions in the machining process: one constantly keeps the cutting wheel working surface free of chips of machined material and the other is constantly ready to true the cutting wheel and to expose new granules out of the bond when needed.

Tool electrode 3, which maintains the cutting ability of the wheel during the machining process, consists in the following. The greatest gap δ_n a resistance arc discharge cannot jump is set between the cutting wheel's current-conducting bond 2 (Fig b) and the working surface of tool electrode 3, which is connected to the direct current terminal. The gap is regulated by a sensor and is kept constant by radial feed s_r, which compensates the linear wear of the tool electrode.

After cutting wheel granules 9 have been worn from the cutting area, chips 8 of machined material remain between them. Some of the chips are pressed between the grains and some are held by inertial and cohesive forces. Initial gap δ_n is reduced to working size δ_r, where erosion discharges are generated to remove the adhered chips and expose fresh cutting granules. Thus the chips make possible the constant generation of self-igniting resistance arc discharges in the cutting wheel dressing area and erosion fracturing of the bond does not occur. The lubricant-coolant fed from nozzle 7 (Fig a), removes the electrical discharge fracturing products.

As the cutting wheel granules become dull and their falling out activates electrode 6 (Fig c), it dresses the wheel until fresh granules in the bond are exposed. The sensor sends a command to the tool electrode to switch on approach feed s_d. The gap decreases to working value δ_r and erosion discharges are generated between the bond and the surface of dressing electrode 6. The fracturing of bond 10 exposes grains 9 to value h, which depends on specific machining conditions and the properties of the cutting wheel. The hardness of the material being machined greatly influences the selection of value h: the harder it is, all other conditions being equal, the less the extent of exposure of the granules, on which machining productivity depends.

Constant radial feed s is transmitted to electrode 6 during erosion fracturing of the cutting wheel bond to compensate for linear wear on the electrode and keep its working surface in the required condition. After the granules have finally been exposed (to extent h), the feed approach command is sent to the truing electrode, which keeps the wheel in cutting condition by removing chips of machined material. During the machining process, the layer of chips between the granules are constantly being filled up with new chips, which is why it should be considered that the tool electrode is constantly dressing the cutting wheel and keeping it in cutting condition. The other electrode is always in a state of readiness to dress the cutting wheel and is activated only in certain conditions.

The cutting wheel dressing method which has been devised greatly increases the productivity of the parts machining process. When D16 and V95 aluminum alloys were cut with 2726-0638AS6250/200 100M1-type diamond cutting wheels, the truing operation was performed stably (at a source voltage of 10...16 V). There was little wear on the dressing electrodes since they were not cut by the cutting wheel granules. The stability of the cutting wheel increased 2.5-fold compared to machining with a single dressing electrode. Nor were there any scratches, burrs or other defects on the machined surface.

UDC 621.867.42

Flexible Feed Mechanisms Discussed

18610546a Moscow MASHINOSTROITEL in Russian No 5, May 89 pp 18-19

[Article by B. M. Gevko, doctor of technical sciences and M. I. Pilipets under the "Mechanization and Automation of Production" rubric: "Flexible Feed Mechanisms"]

[Text] Flexible screw conveyers are simple and convenient when used to operate feed mechanisms or haulage units. They have a number of advantages over other similar devices: they are air-tight, simple to manufacture, transportable, highly productive and operationally reliable.

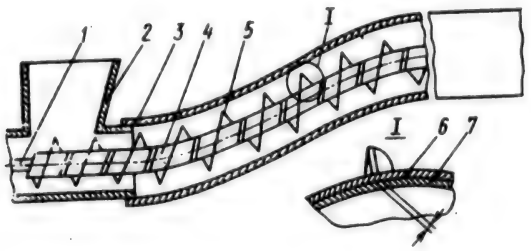

Figure 1.

The Ternopol branch of the Lvov Polytechnical Institute has developed a number of flexible screw mechanisms. Figure 1 shows a screw conveyer (a.s. 1315369), which contains flexible shell 3 with loading hopper 2. A working element in the form of a flexible shaft 4 is mounted inside the shell. The shaft consists of outside (6) and inside (7) cylindrical spiral screws coiled in opposite directions. The flexible screw--spiral 5--is welded through two or three turns in the middle of the turn of the outside cylindrical spiral. The direction of its turns matches that of the coil of the outside screw spiral.

The outside and inside cylindrical screw spirals are joined to each other at the point at which they are joined to drive 1 and at the discharge at the unloading portion of the conveyer. The interval of the flexible spiral equals the interval of the turn of the outside and inside cylindrical screw spirals.

When the drive shaft is activated, the material being transported from the loading hopper is moved by the flexibe spiral and the flexible shaft to the unloading portion, where it spills out. In the process of the

transport operation, the flexible and outside (6) cylindrical screw spirals operate by twisting and the inside (7) cylindrical screw operates by untwisting. Since the inside cylindrical spiral untwists to the point of its limiting value, it restricts the twisting of the outside cylindrical screw spiral. This increases the torsional rigidity of the working organ by several times. The working element derives its flexibility from gap b between the turns of cylindrical spirals 6 and 7. The size of the gap falls within 2...6 mm for flexible shafts with an outside diameter of up to 30 mm.

The cylindrical spirals can be made of coiled steel ribbon using 08kp and other grades of steel with a thickness of from 0.5...1 mm.

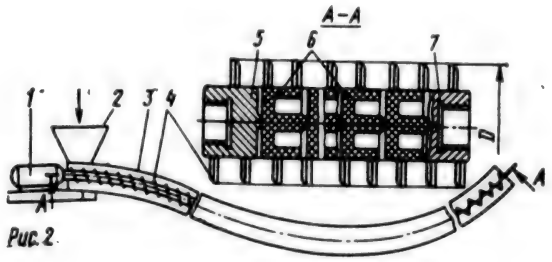

Figure 2.

Figure 2 shows a flexible screw conveyer with a flexible shaft made in the form of individual plastic elements (a.s. 1346530). It consists of electric motor 1, loading hopper 2, flexible shell 3 and screw spiral 4. The latter is made in individual sections joined by coupling halves 5 and 7. The direction of the screw spiral should be such that both coupling halves perform a screwing action to transport the load. Between the coupling halves, there are plastic elements 6 with spherical protrusions which come in contact with matching recesses in the following elements. The length of these sections are determined by structural or production conditions.

To attach one of these sections to the screw spiral, coupling half 7 is welded on one side. This half has an outside diameter equal to the internal diameter of the screw spiral. In its free state, the internal diameter of the screw spiral is 0.5...2 mm less than the outside diameter of plastic elements 6. In order for the plastic elements to fit into the spiral, the latter must be unscrewed a little so as to increase its interior diameter. After the plastic elements have been mounted, the second coupling half 5 is welded to the other side of the section, which joins it to the adjacent section.

In order for the screw conveyer to operate normally, the plastic element must be 1.5-2-fold longer than the screw interval. This relationship will prevent the assembled elements from separting in the course of any radial flexure which may occur. The distance of pitch T of the flexible screw band is taken from condition $T = (0.5...0.7)D$, where D is the outside diameter of the spiral.

The conveyer sections can differ from each other in the thickness of the spiral. Here, the thickest worm conveyer is attached to the electric motor shaft and the thicknesses of the worm conveyers of the following sections is reduced. The last section has no flexible shaft because the thickness of the spiral is equal to the thickness of the first section, which is attached to the electric motor shaft. This design provides a roughly identical safety factor.

The rotation of the electric motor turns the flexible worm conveyer, whose individual elements operate by twisting, the extent of which is limited by plastic inserts. This helps the conveyer load better.

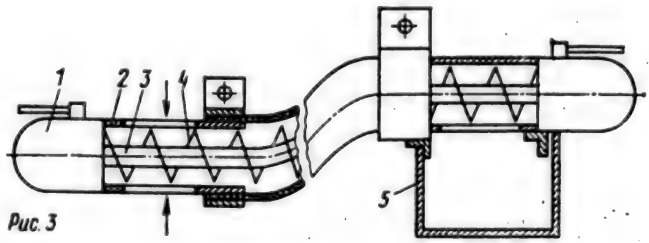

Figure 3.

The flexible worm conveyer (a.s. 1344697) shown in Figure 3 consists of electric motor 1 attached to tube 2. Flexible worm 4 is mounted inside the tube. The worm is welded to flexible cable 3 by turns 2...3. The cable is rigidly attached to the electric motor drive shaft. To improve the operating conditions, the second end of the flexible worm is attached via a thrust bearing mounted in tube 2. The material to be transported enters the working zone (arrows) and is caught up and fed into the loading hatch by auger 4 and thence to holding bin 5.

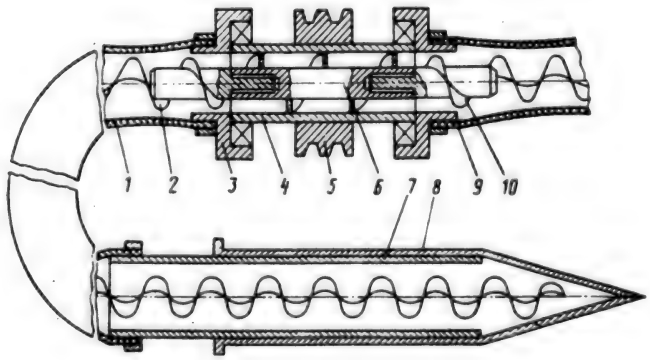

Figure 4.

Figure 4 shows a diagram for a centrally-driven flexible conveyer (a.s. 1348268), which allows the length of the flexible conveyer to be increased. It contains drive sheave 5, which is rigidly mounted on support tube 4, into which the central screw spiral attached to shaft 6, is inserted.

The support tube is mounted through the bearings mounted in housing 3. The stepped shafts, upon which flexible augers 2 and 10 are cantilevered, are attached through a threaded joint to shaft 6. Flexible shells 1 and 9 are attached to the housing by collars. The loading section consists of quill shaft 7, to which the end of flexible housing 1 and cover 8 are attached. The latter is cylindrical and has a connector adapter made of lobes curved in alignment with the axis of the auger and forming a polyhedral cone which protects the end of the auger from damage while in transport position.

When the unit is in operation, the cover, along with the quill shaft, are inserted into the bulk material being transported to a certain depth. The cover is then pushed onto the quill shaft, which action uncovers its lobes. The cover should be moved far enough to ensure that the unit is able to load continuously during operation. When the electric motor is switched on, rotation is imparted by sheave 5 to support tube 4 and augers 2 and 10. As it is being transported, the bulk material passes through the central portion of the flexible transporter under the pressure of the material, which pressure is created by auger 2, after which it is fed to the discharge vent by auger 10.

The most important structural elements of the flexible worm conveyers discussed here are the pitch of the spiral and the minimal extent of the radius of the arc of curvature. These parameters have a considerable effect on the course of the production process and the reliability and durability of the mechanisms involved. Research results have shown that the pitch of the spiral should be within (0.4...0.7) D, where D is the outside diameter of the spiral, and the minimal radius of the arc of the curve should be within (10...15) D. The pitch must be reduced in order to reduce the radius of the arc.

The flexible worm gear mechanisms which have been developed can have broad practicle application in industry and agriculture with regard to mechanizing labor-intensive production processes involving moving bulk materials.

UDC 621.778.23.06

Sheet-Bending Machine Examined

18610547a Moscow MASHINOSTROITEL in Russian No 6, Jun 89 p 7

[Article by V. P. Slobodyanyuk and M. Ye. Kats: "The Sheet-Bending Machine"]

[Text] VPTIenergomash [All-Union Planning-Design Insitute of Power-Engineering Machinery] has worked up technical documentation (a. s. 837473) and constructed a machine for using heat from high-frequency current to bend irregularly-shaped streetcar rails, channel beams, I-beams, angle-iron and bars, as well as steel tubes up to 465 mm in diameter with no filler, and using the appropriate interchangeable attachments.

The bending technique consists in heating a narrow area of the section within an electromagnetic inductor field to a temperature of 1,000° C. Under the effect of the longitudinal and transverse forces applied to the workpiece, a simple bend is formed in the heated area. The workpiece moves through, and the heated area moves along the section, which is flexed at each section. The total of these bends forms a bend of the prescribed radius.

The electric currents are distributed non-uniformly along the thickness of the section, and are concentrated in vortices in the upper layers of the metal, which vortices amount to practically zero deeper in the metal. The workpiece cross-section is heated to a prescribed depth in the metal, and the heat usually penetrates to roughly 6.7, 12 and 19 mm for steel at frequencies, respectively, of 8,000, 2,500 and 1,000 Hertz. Over 85 percent of the heat energy is released at this depth.

Workpieces having a metal thickness in excess of the depth to which the heat penetrates are commonly bent in industry. The internal layers are heated by metal heat conductivity. The bending regimes are selected experimentally.

When bent with induction heating, the metal of the workpiece is sequentially heated to a high temperature and intensly cooled with water from the induction heater sprayer. When necessary, heat treatments can be performed on the machine (for example, quenching of streetcar rails).

The workpiece section is marked and the workpiece is set in the machine, secured in the carriage by a clamp and held on the guide rollers by a positioning mechanism. The pressure roll presses on the workpiece section, bending it in the heated area. The radius of the bend depends on the position of the pressure roll, and the transition from one radius to another is made without interchangeable attachments. A template or a radius-angle gauge are used as a control. The lateral feed mechanism moves the pressure roll along the carriage. The longitudinal feed mechanism moves the pressure carriage with the bent section along the bed. A high-frequency transformer, with a high-frequency current induction coil secured to it, is mounted in a holder on the guide roll carriage. The beginning of the bend must be located beneath the induction heater. Water is used to cool the bending machine assemblies and the high-frequency current device.

When the workpiece section is heated to the requisite temperature, the longitudinal and lateral feed is switched on from the control panel. When the pressure roll has moved the section the prescribed distance, the section stops moving. The bending continues in a single longitudinal feed until the required bend angle is achieved, after which the machine switches off and the workpiece section is removed from the machine.

The items to be bent are made of M75 and 20 carbon steels. The minimum bending radius is 2,000 mm for sections and 2 D for pipe. The machine puts out 10.8 running meters per hour. The machine, without the high-frequency current device, has a mass of 26 t.

It is recommended that a monorail with a motor hoist be mounted on support arms along the axis of the machine to facilitate maintenance. It is a good idea to set up a bin for the large workpieces which are to be bent behind the machine. The configuration of the bending mechanism allows the bent workpieces to be stored alongside the bending machine. The monorail must be long enough to ensure that workpieces can be fed from the bin to the machine and removed from the machine, and that the finished output can be stockpiled.

The probable economic effect of introducing the bending machine with high-frequency current heating is R75,000, thanks to the reduced labor intensiveness of the bending operations and the increased cost of irregularly-shaped products in the process of operation.

UDC 621.757.06
621.774

Multi-Wall Pipe Assembly Described

18610547b Moscow MASHINOSTROITEL in Russian No 6, Jun 89 p 11

[Article by V. A. Mikhaylov under the "Developed--Introduced" rubric: "Assembling Multi-Wall Pipe"]

[Text] Metallic hoses and compensators, the flexible portion of which is manufactured of hydroformed multi-wall pipe, are used in a number of industrial sectors.

The carrying capacity of multi-wall compensators depends on the quality with which multi-wall pipe is assembled. The latter is assembled from pipe blanks primarily by two methods: by "pulling" the inside pipe into the outside pipe (for pipes longer than 2 m) and by "pushing" the inside pipe into the outside pipe (for pipes from 0.5...2 m long).

In this type of assembly, the pipe walls coming into contact create nadirs, scratches and galling in the space between the walls, thus shortening the service life of the metal hoses and compensators.

In order to improve the quality with which these pipes are assembled, a device has been developed which makes it possible to assemble them without defects. It ensures that one pipe enters the other without their walls touching because of the inside blank having its diameter reduced in the manufacturing process. The device allows the walls of the pipe to operate during elastoplastic bending. The nature of the deformations, depending on the radius of the bend in the walls of pipes with a nominal diameter of D_y=70...350 mm, is shown in the table.

a Условный диаметр D_y, мм	b Оптимальные радиусы изгиба профиля R, мм	c Толщина стенки трубы S, мм	d Относительный радиус изгиба $r = \frac{R}{S}$
350	65	0.3	183.3
300	48	0.3	160.0
200	32	0.3	106.6
175	28	0.3	93.3
150	24	0.3	80.0
125	20	0.25	80.0
115	18	0.25	72.0
100	16	0.2	80.0
90	14	0.2	70.0
80	12	0.18	66.0
70	10	0.18	55.5

Key: a--nominal diameter D_y, mm; b--optimal bending radii of shape R, mm; c--pipe wall thickness S, mm; relative bending radius

It follows from the table that when manufacturing multi-wall pipes of diameter D , equal to 70...350 mm, the wall material is in a state of elastoplastic flexure, since the relative radius of bend

$$r = \frac{R}{S}$$ is not greater than 200.

Fig 1

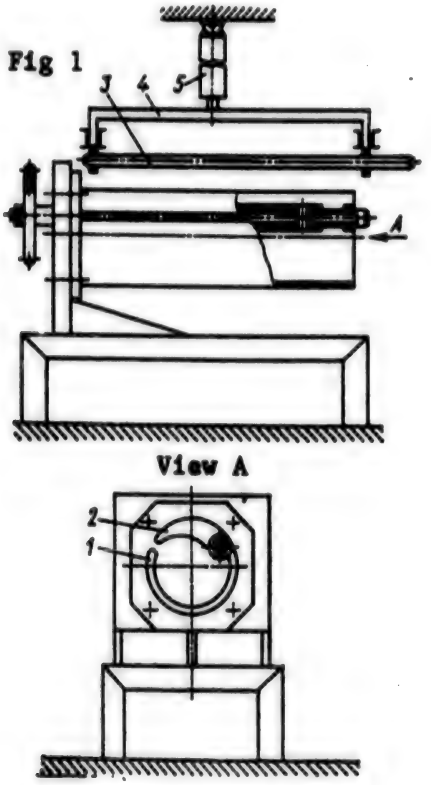

The device is made up of housing 1 (Fig 1) with draw spike 2, rod 3, slide bar 4 and hydraulic cylinder 5.

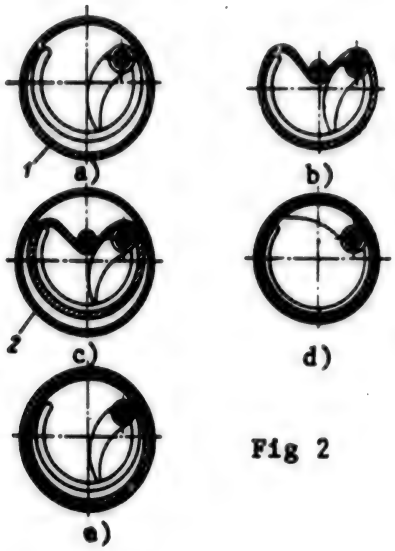

Fig 2

Inner blank 1 (Fig 2, a) moves freely (without touching the walls) within the device's housing. The movement of the rod deforms the wall of the inner blank (Fig 2, b), thus reducing the pipe's diameter by 10...15 percent. In this state, the pipe is held in the housing by the rod. The slide bar is raised to the initial position and outer blank 2 moves freely (without touching the walls) (Fig 2, c). After the rod is removed by the draw spike, the initial cylindrical shape of the inner pipe is restored (Fig 2, d). The draw spike then returns to its initial position (Fig 2, e) and the assembled dual-wall pipe is easily removed from the housing.

When assembling pipes with a large number of walls, the assembly sequence is retained. Multi-wall pipes in diameters of 125, 150 and 174 mm were assembled on the experimental device with no damage. The productivity of this method of assembly was equal to that of other assembly methods.

UDC 621.865.8-236.58-8

Flexible Positioning Systems Examined

18610547c Moscow MASHINOSTROITEL in Russian No 6, Jun 89 pp 12-13

[Article by A. N. Makarov, I. M. Kutlubayev and A. O. Kharitonov, candidates of technical sciences, under the "Mechanization and Automation of Production" rubric: "Positioning Systems with Flexible Tractive Elements"]

[Text] Historically, the design sense, as it relates to devising manipulating systems, has travelled the path from the most elementary cable positioners for excavators and gantry cranes to complex multi-link systems employing hydraulic devices, electric machinery, geared mechanisms etc.

Why has such a broad spectrum of manipulator designs sprung up? What caused the developers to turn away from the flexible tractive elements which had previously been the most popular for performing essentially the same motions? One of the main reasons was the fact that independent movement of the positioner links was easier to achieve with hydraulic cylinders, electric motors etc. In other words, it was simpler to use these designs to isolate movements in the positioner joints. However, equipping positioner links of this type with such devices greatly increases the mass of their moveable parts. In addition, the positioning accuracy of the grippers on these positioners is provided by controlling supports which restrict the limiting position of pairs of links to each other. These significant flaws have become a peculiar way to pay for the simplicity of isolating the movements of manipulators provided by installing activators on the moveable links. Nevertheless, the development of manipulator systems employing flexible tractive elements to drive the links has been held back by precisely the fact that the problem of isolating their motions has not been solved.

It should be mentioned that there have been attempts to devise cable positioners in which the motions are isolated by tracking the changes in the lengths of the cables between the links in the positioner control system when their relative positions are changed. However, devising positioner systems with more than three moveable links operating in this manner has turned out to be inefficient because it so greatly complicates the control system.

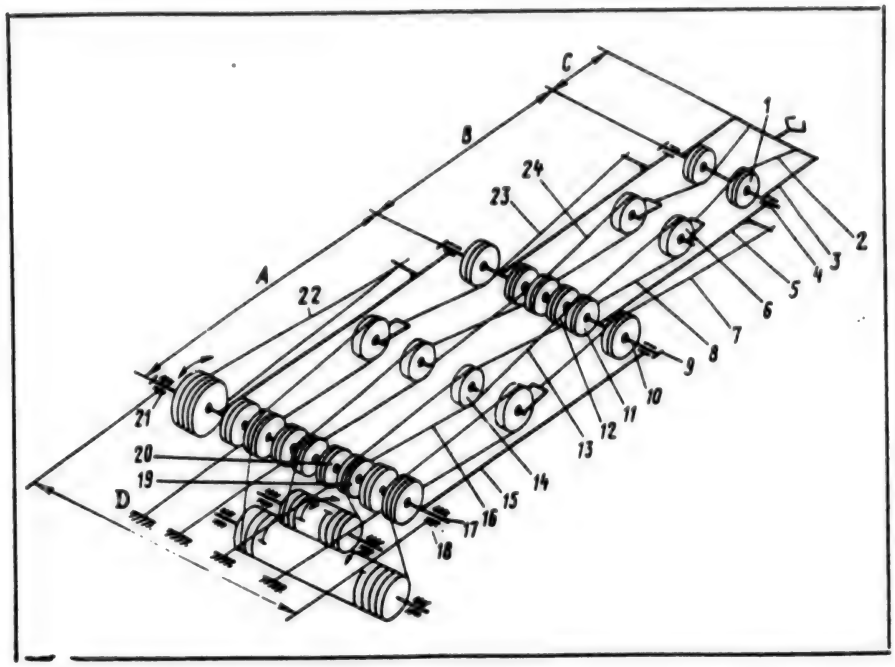

This article examines the design of a positioner driven by flexible tractive elements, thus kinematically isolating the motions in the joints. The figure shows a kinematic diagram of a positioner with three moveable links 15, 5 and 3 and base 18. The links are connected sequentially between themselves and the base by joints 17, 9 and 4. Mechanical drives 16, 3 and 2 and their cables, which move the links forward and back, are positioned above the links. Mechanical drives 8 and 24 move link 3, mechanical drives 7 and 23 move link 5 forward and back, and mechanical drive 22 moves link 15. Each mechanical drive is sequentially connected through a system of cable block pulleys.

The originality of this kinematic isolation of movement is protected by patent # 1306705, issued for the positioner structural arm. This mechanism functions as follows.

When link 15 needs to be rotated relative to base 18, counter-clockwise for example, the position of link 3 does not change relative to link 5 nor that of link 5 relative to link 15: the individual drive of the latter link is activated. Motion is imparted from the drive to the cable attached to link 15 by mechanical drive 22, the tension for which is produced by the torque around axle 21. Acted on by this torque, link 15 moves counter-clockwise, and as this occurs the individual drives for the remaining four mechanical drives are disengaged.

When acted upon by link 15, which is rotating counter-clockwise, cable length 16, held between the bases by pully plocks 20 and 19, unreels from the latter. This increases the length of cable length 16 and, running around base pulley block 20 in the opposite direction (to the length of cable running around block 19), it winds onto block 20. Because of the equal diameters of the base blocks, the length of the part

of the cable unreeled from pulley 19 is equal to the length of the portion of the cable winding onto block 20. Here, idler pulley 14 rotates counter clockwise and its axle remains stationary relative to link 15, which keeps the ends of cable 13 stationary relative to link 15, and consequently the position of link 3 remains unchanged relative to link 5. Here, the drive for mechanical drive 8 is disengaged. Thus, when link 15 rotates relative to base 18, the relative position of links 5 and 3 has not changed, which results in the kinematic isolation of the movements.

When it is necessary to rotate link 3 relative to link 5, counter-clockwise for example, the motor for mechanical drive 8 is engaged. As this occurs, motion in the direction away from axle 21 is imparted to the end of cable 16, which is connected to the drive output element. Base pulley 19 rotates counter-clockwise, idler pulley 14 rotates clockwise and its axle approaches axle 21 because the second end of cable 16 is held stationary. The ends of cable 13, which are attached to the axle of pulley 14, move toward axle 21. This rotates pulleys 12 and 11 simultaneously. The latter rotates counter-clockwise, and as this occurs cable 13, which is held between pulleys 11 and 12 and idler pulley 6, decreases in length. Without rotating, pulley 6 moves with its own axle toward axle 10. The end of cable 2, which is attached to the axle of pulley 6, also moves toward axle 10. This results in main pulley 1 rotating clockwise and reeling in a portion of cable length 2, which is between pulley 1 and the point where the cable is attached to link 3. This rotates the latter counter-clockwise relative to link 5. Activating the drive for link 3 smoothly lengthens mechanical drive 24, which is associated with the rotation of link 3. As this occurs, the amount mechanical drive 8 is shortened, which drive is located above the moveable links, is equal to the amount the similar portion of mechanical drive is lengthened, which allows the forward and reverse motion of the link to be driven by a single drive.

This article examines only two of the possible movements of the positioner's links. This design for kinematic isolation of motion can be used on positioning systems with more than three moveable links and where the angles for changing the mutual position of the links can be as much as 300...310°. Moreover, in this instance the movements are kinematically isolated regardless of the type of flexible tractive element used, be it a cable, chain, belt etc. The proposed design was realized in a model of a cable positioner with three moveable links. The following dimensions were used: A=240mm, B=200 mm, C=90 mm, D=120 mm and the cable diameter was 1.2 mm. Testing the models in laboratory conditions showed that this design provides the limiting value for the ratio of the mass of the load being moved to the mass of the moveable parts of the manipulator, which is 3.2, which greatly surpasses the same indicators for series-produced positioners. Here, the output of the drive motors for links 15, 5 and 3 is 8, 8 and 10 W respectively. Preliminary stretching of the cables to 70 N makes the manipulator structure taut, enhancing its positioning accuracy, which came to an accuracy of 1.2 mm in laboratory conditions.

The prospects for developing positioning systems which employ flexible tractive elements can be extremely encouraging, thanks to: the presence of a well-developed industrial base, which produces a sufficient volume of components for this design at relatively low cost; the wide range of uses for these manipulators, which in fact equals that of existing load-lifting mechanisms with flexible tractive elements; the stability of quality indicators and the operational reliability of of the system, independent of changes of such environmental parameters as temperature, pressure etc, in light of the fact that the drives for each moveable link have mechanical drives which are direct and of equal length and are under equal tension from the mechanical drives, which mutually compensate for the linear elastic deformations of the flexible tractive elements; and thanks to the link drives for the stationary base having been removed, which enhances the positioner's operational reliability while simultaneously reducing the system's inertia.

Of all the known designs for a positioning system, this one comes closest by virtue of its structure and layout to the best manipulator design existing in nature--the human hand--which the developers used as a starting point in formulating the idea for creating a manipulating system employing flexible tractive elements.

UDC 621.952-229.27-231.215

Self-Centering Safety Chuck Developed

18610547d Moscow MASHINOSTROITEL in Russian No 6, Jun 89 p 45

[Article by G. P. Urlapov, candidate of technical sciences, under the "Developed--Introduced" rubric: "The Self-Centering Safety Chuck"]

[Text] One flaw in the existing designs for safety chucks used to secure chipless taps is the considerable radial wobble of the working portion of the tap when the machine-tool spindle is rotating freely. When radial-drilling machines are used to make threaded holes in large workpieces, this wobbling makes it difficult to insert the tap into the pre-drilled hole while in motion, i.e., without stopping the rotation of the machine spindle. In order to eliminate this flaw, the Scientific-Research Threaded-Tools Laboratory of the Vinnitsa Polytechnic Institute has developed and initiated production of a self-centering safety chuck designed to secure chipless taps which cut M6 to M16 threads.

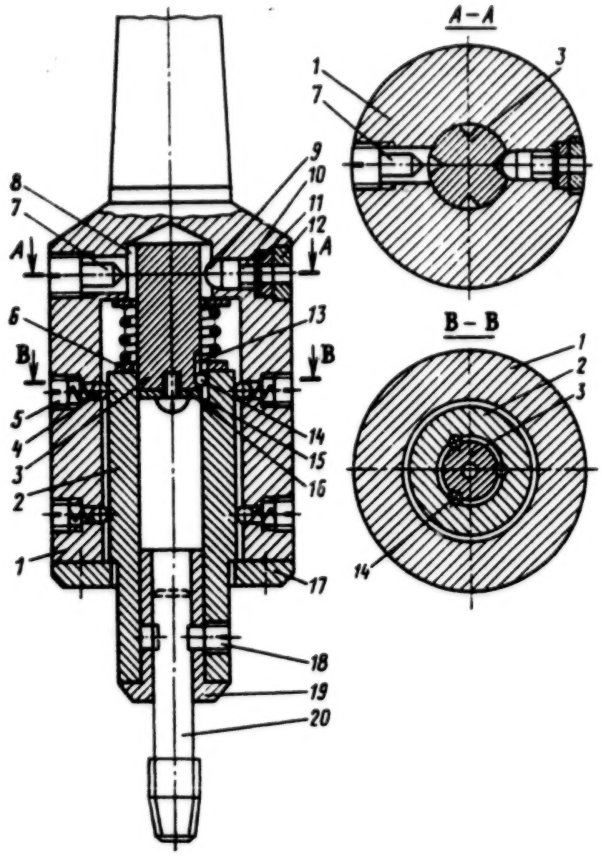

Keeper 2 and guide 3 are located in chuck housing 1. Four longitudinal grooves 8 have been cut into the upper part of the guide, and longitudinal semicircular grooves 13 in the lower part. The spherical surface of punch 10, which is mounted in a radial opening in the housing, fits into one of the guide's longitudinal grooves. The cylindrical end of the punch rests in safety plate 11, which is set in the die and tightened by tubular screw 12, which is screwed into the housing. Balls 14, which also fit into corresponding semicircular grooves 15 of the keeper are set in the guide's longitudinal semicircular grooves. Washers 6 and 16 keep them from falling out of the grooves. Interchangeable bushing 19 is inserted into the keeper opening from below by the internal opening which forms the base for the tail end of tap 20. Two screws 18, which fit into square notches in the shank of the tap (or rest in a side of the square), keep the tap from falling out of the interchangeable bushing, and the keeper itself is prevented from falling out of the chuck housing by cover 17, which is screwed to the chuck housing.

In order to eliminate radial wobble in the working portion of the tap there are eight radial openings in the housing, into which are set spring-loaded balls 4, which are adjusted by screws 5.

The chuck is set into the radial-drilling machine, the tap is inserted into the opening of the interchangeable bushing and held there by screws

18. While the drilling machine spindle rotates slowly, an indicator head is used to determine the extent of radial wobble of the working portion of the tap and when necessary to eliminate the wobble with adjusting screws 5. During operation, rotation is imparted from the chuck housing through the spherical surface of punch 10 to the guide, and thence via ball 14 to the keeper. Rotation is imparted from the keeper through screws 18 to the tap.

When a workpiece is mounted on the drilling machine table to be machined, the axis of the pre-drilled hole can shift or be misaligned relative to the axis of rotation of the tap. Should this occur the keeper, thanks to the clearance with which it is set into the chuck housing, can be moved and set somewhat at an angle to the axis of the chuck which corresponds to the axis of the hole in the workpiece. After the tap is screwed out of this hole the keeper, acted upon by spring-loaded balls 4, assumes its initial position.

Threading torque can greatly increase if the diameter of the hole beneath the tap narrows or the tap is resting on the bottom of the blind hole. In this instance, when acted upon by the radial force generated in the area where punch 10 comes in contact with the guide, the punch with its cylindrical end presses on the safety plate, and its spherical end comes out of the guide's longitudinal groove. The chuck housing begins to turn freely relative to the stationary guide, and keeps the tap from breaking. In order to back the jammed tap out of the hole, screw 7 enters by its conical end into one of the longitudinal grooves in the guide, the drilling-machine spindle is put into reverse rotation and the tap is backed out. Then screw 7 is backed off and the safety plate is replaced.

Correctly calculating the thickness of the safety plate ensures that the chuck's safety device will operate reliably, which can totally eliminate breakdowns of chipless taps during operation. The design's spring-loaded balls 4 allow the keeper and working portion of the tap to retain their intial position (without wobbling) during operation. This will shorten the time spent on aligning the tap and the hole.

IN BRIEF

Specialists from the TsNIITmash NPO [Central Scientific-Research Institute of Technology and Machinery Manufacture], working together with colleagues from the UkSSR Academy of Sciences' Physico-Mechanical Institute imeni G. V. Karpenko, have developed a new method for quality control of castings and welded joints in machine building. An x-ray machine is used to investigate the structure of the metal, and the data are transmitted to a television monitor with a digital data-processing system and an electronic memory.

* * *

The Biyskiy Machine-Building Plant, of USSR Gosagroprom, has initiated production of a compact and economical device for spraying metals. It

can be used effectively to restore worn parts on agricultural machinery in any agricultural shop. The Altay machine-builders have manufactured more than 30 of these devices this year.

- END -

END OF FICHE

DATE FILMED

27 Nov. 1989